Transient Characteristics of Continuous Extraction with Agitation

H. K. STAFFIN and JU CHIN CHU

Polytechnic Institute of Brooklyn, Brooklyn, New York

Process control in the chemical industry has been accomplished with off-on, proportional, integral, or reset controllers to provide the required compensation in the control loop. In recent years advances in the field of special purpose analog devices has made it possible to apply considerably more sophisticated compensation functions to achieve superior control performance.

To engineer a feedback control system and determine the required form of compensation to meet process requirements some form of process characterization is necessary. For systems which can be described by linear differential equations the transient response of the system expressed as a transfer function offers a convenient method of characterization. In addition to the benefits of transient analysis in design of process control systems, the data obtained are extremely useful in formulating a process analog simulation permitting the study of process behavior with an analog computer.

Transient analysis of a system involves studying the response of a system to known disturbances in an experimentally controlled environment. Early applications of this type of analysis were by Rosen and Winsche (*16*) in a theoretical kinetic study of gas chromatography and by Diesler and Wilhelm (*7*) in the study of diffusion in beds of porous solids. More recently transient analysis has been applied to many phases of engineering including response of heat exchangers (*10, 13*), reactors (*6, 12, 11*), distillation columns (*3, 18*), flow through packed beds (*8, 14*), and many others.

The objectives of this investigation were to study the concentration transient response characteristics for the diffusion of a given solute between two liquid phases in an agitated contactor and to relate the transient response characteristics to the properties of the system and the operating conditions to permit prediction of transfer functions for design purposes.

In this study a single agitated vessel was operated as a continuous contactor in a liquid-liquid extraction. The concentrations of solute in the feed streams to the contactor were varied by step changes, and the concentration responses of the two phases in the contactor were determined by analysis.

H. K. Staffin is at Stevens Institute of Technology, Hoboken, New Jersey.

MATHEMATICAL ANALYSIS

The characteristics of a linear system with respect to a given property are completely determined by the response of the system to changes in the given property. A physical system is said to behave linearly over a specific range of one of its variables if its behavior in the range can be described by a linear differential equation. Many systems encountered in chemical processing are nonlinear; however over relatively small ranges they frequently can be approximated by linear differential equations. Of particular interest in the field of dynamic analysis are systems described by linear differential equations with time invariant coefficients. The general linear differential equation with time invariant coefficients can be written in operator form as

$$\Phi(D)\theta_0(t) = \xi(D)\theta_i(t) \tag{1}$$

The function most frequently used to describe a system of this type is the transfer function $H(s)$, defined by

$$H(s) = \left.\frac{\xi(D)}{\Phi(D)}\right|_{D=s} \tag{2}$$

For systems which are at rest before the input disturbance $\theta_i(t)$ is applied, commonly referred to as *initially inert* systems, it is readily shown that

$$H(s) = \frac{\theta_0(s)}{\theta_i(s)} \tag{3}$$

Thus the response of the initially inert system to a known disturbance can be used to establish the system transfer function, which in turn completely characterizes the response of the system to any known disturbance. Of particular interest in the application of these principles to a real system are unit impulse $\delta(t)$ and unit step $u(t)$ input signals.

The unit impulse function is defined by

$$\begin{aligned} \delta(t) &= 0\ , \quad t < 0 \\ \delta(t) &= \infty, \quad t = 0 \\ \delta(t) &= 0\ , \quad t > 0 \end{aligned} \tag{4}$$

$$\int_{-\infty}^{+\infty} \delta(t)\,dt = 1$$

The unit step function is defined by

$$\begin{aligned} u(t) &= 0\ , \quad t < 0 \\ u(t) &= 1.0, \quad t \geq 0 \end{aligned} \tag{5}$$

It is not possible to generate and apply the unit impulse or unit step functions because real systems cannot be changed over a zero time interval but are actually changed over short time interval ϵ; however these functions may be approximated within a required precision range by the signals $\delta_\epsilon(t)$ and $u_\epsilon(t)$ respectively. Obviously the smaller that ϵ can be made, the closer the approximation, and in the limit as ϵ approaches zero

$$\lim_{\epsilon \to 0} \delta_\epsilon(t) = \delta(t) \tag{6}$$

$$\lim_{\epsilon \to 0} u_\epsilon(t) = u(t) \tag{7}$$

If the input signal $\theta_i(t)$ [in Equation (1)] is a unit impulse function $\delta(t)$, then the output function $\theta_0(t)$ is the unit impulse response function $g(t)$. Since the Laplace transform of a unit impulse function is unity, Equation (3) yields

$$H(s) = \frac{G(s)}{\delta(s)} = G(s) \tag{8}$$

Therefore the transfer function $H(s)$ of the system can be obtained by taking the Laplace transform of the system unit impulse response, or

$$H(s) = \int_{0-}^{\infty} g(t)e^{-st}\,dt \tag{9}$$

A convenient method for obtaining the transfer function from impulse response data is to first take the Fourier integral of the impulse response giving the frequency response function $\overline{H}(jw)$ as follows:

$$\overline{H}(jw) = \int_{0-}^{\infty} g(t)e^{-jwt}\,dt \tag{10}$$

The settling time of the process, designated T_s, is defined as the time required for the process to settle within 2% of its original value after being disturbed by a unit impulse. Since the value of $g(t)$ after T_s is approximately zero, Equation (10) may be approximated by

$$\overline{H}(jw) = \int_{0-}^{T_s} g(t)e^{-jwt}\,dt \tag{11}$$

By Eulers identity Equation (11) may be written as

$$\overline{H}(jw) = \int_{0-}^{T_s} g(t)\ (\cos wt - j \sin wt)\,dt \tag{12}$$

$$= \int_{0-}^{T_s} g(t) \cos wt\,dt - j \int_{0}^{T_s} g(t) \sin wt\,dt \tag{13}$$

Therefore the impulse function $g(t)$ enables the determination of the frequency response function $\overline{H}(jw)$ for any angular frequency w. Application of Equation (13) for various values of w permits plotting the frequency response function over the range of frequencies of interest, the most useful representation of these values being the well-known Bode diagram. This procedure was readily accomplished with a special purpose analog computer.

To compute the real and imaginary parts of $\overline{H}(jw)$ the following analog diagram (Figure 1) was used to simulate the mathematical equation for $\overline{H}(jw)$, Equation (13).

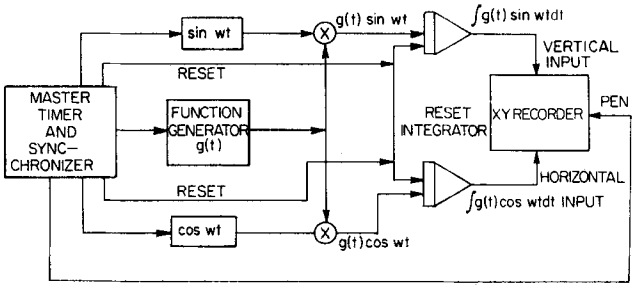

Fig. 1. Fourier transform computation.

The unit impulse response function $g(t)$ was generated on an adjustable function generator. Multipliers were used to form the product $[g(t) \sin wt]$ and $[g(t) \cos wt]$. These product functions were then integrated for a time interval T_s. Since the integrators were reset, or cleared, at $t = 0$, the integration outputs at time T_s yielded the real and imaginary parts of $\overline{G}(jw)$. The output of the cosine generator chain was plotted on the X axis of a recorder and the output from the sine generator chain plotted on the Y axis; thus one data point of $\overline{H}(jw)$ was obtained at time T_s. Changing the frequency of the sine and cosine generators and repeating the procedure gave the other data points over the frequency range of interest.

There are a number of mathematical techniques (*2, 4, 9, 19*) that permit going from the Bode diagram for $\overline{H}(jw)$ to an analytical expression for the system transfer function. For relatively low-order systems, second or third, the properties of the Bode diagram itself can be used to fit the graphical representation of the frequency response function with an analytical form for the transfer function (*2, 9*). The results obtained in this study all suggested low-order differential equations; therefore this technique was satisfactory.

This mathematical analysis procedure permitted characterization of the diffusion process once the impulse response function $g(t)$ was determined. Since the system was defined on the basis of input and response functions being associated with bulk concentrations inside the agitated vessel, it was impractical experimentally to make impulse or step changes in the input function to the system. It was feasible however to make step changes in the feed streams to the vessels and measure the response of the bulk compositions inside the vessel to these changes. These responses were then regarded as the input signal to the diffusion system and therefore were not step or impulse functions but concentration functions of time which could be measured experimentally.

The problem then was, basically: given any input function $\theta_i(t)$ to the diffusion system and its corresponding output, find the system impulse response function to permit application of Equation (13). The relationship between these functions, for an initially inert linear system, is given by the convolution integral

$$\theta_0(t) = \int_0^t \theta_i(\tau)g(t-\tau)\,d\tau \tag{14}$$

This integral is numerically approximated by

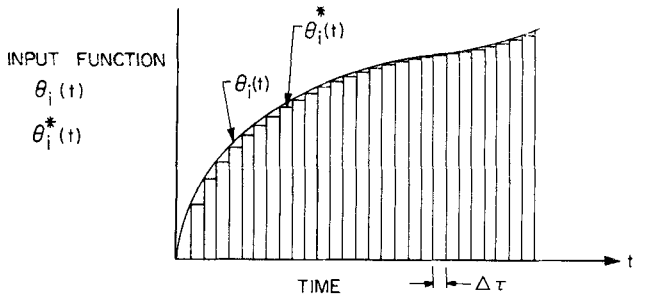

Fig. 2. Approximation of system input function.

$$\theta_0^*(t) = \sum_{k=0}^{t/\Delta\tau} \theta_i^*(d\Delta\tau)g^*(t - k\Delta\tau)\Delta\tau \qquad (15)$$

For convenience the magnitude of $\Delta\tau$ is considered as unity, giving

$$\theta_0^*(t) = \sum_{k=0}^{t} \theta_i^*(k)g(t-k) \qquad (16)$$

Therefore given the input function $\theta_i(t)$ and the unit impulse response function of the system $g(t)$ these functions can be divided into equal segments and approximated as shown in Figures 2 and 3. If the value of the function at each step is written in the form of a polynomial, for example the functions in Figure 2, for $\theta_i^*(t)$

$$\theta_i^*(\Delta t_1) + \theta_i^*(\Delta t_2)Z + \theta_i^*(\Delta t_3)Z^2 + \ldots \qquad (17)$$

and for $g^*(t)$ in Figure 3

$$g^*(\Delta t_1) + g^*(\Delta t_2)Z + g^*(\Delta t_3)Z^2 + \ldots \qquad (18)$$

Then Equation (16) indicates the approximation function of the system response $\theta_0^*(t)$ given by the coefficients of the polynomial formed by the algebraic multiplication of Equations (17) and (18), or

$$\theta_0^*(\Delta t_1) + \theta_0^*(\Delta t_2)Z + \theta_0^*(\Delta t_3)Z^2 + \ldots =$$
$$(\theta_i^*(\Delta t_1) + \theta_i^*(\Delta t_2)Z + \theta_i^*(\Delta t_3)Z^2 \ldots)$$
$$(g^*(\Delta t_1) + g^*(\Delta t_2)Z + g^*(\Delta t_3)Z^2 + \ldots) \qquad (19)$$

Equation (19) can be used to determine the impulse response of a system from an arbitrary input and corresponding output by rearranging to

$$\sum_{b=1}^{n} g^*(\Delta t_b)Z^{b-1} = \frac{\sum_{m=1}^{p} \theta_0^*(\Delta t_m)Z^{m-1}}{\sum_{r=1}^{u} \theta_i^*(\Delta t_r)Z^{r-1}} \qquad (20)$$

Equation (20) was used to determine the system unit impulse response from the experimentally imposed input

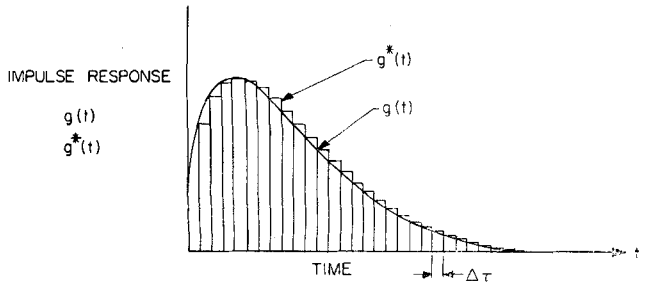

Fig. 3. Approximation of system impulse response function.

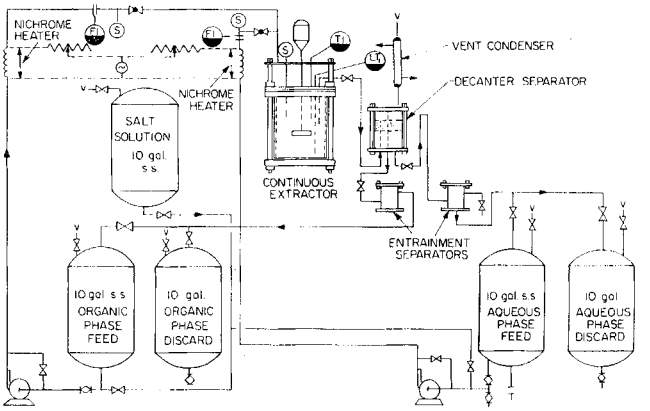

Fig. 4. Mass transfer equipment.

function and corresponding output function. The computation was performed with a digital computer which permitted use of very small approximation intervals giving a very good curve fit.

Equation (13) was then used to determine the Bode diagram of the system with the unit impulse response known.

EXPERIMENTAL EQUIPMENT

The experimental equipment consisted of an agitated tank and the necessary piping, tankage, pumps, and instrumentation to operate the tank as a single-stage continuous extractor. A flow sheet of the experimental equipment is shown in Figure 4.

The organic and aqueous phases were pumped from their respective surge tanks through flow meters to a junction point just before the entrance to the extractor. In the extractor the two-phase system was continuously agitated and maintained at constant level by continuously overflowing to a decanter. The phases were separated in the decanter, each passed through an entrainment separator, and returned to their respective surge tanks. This flow pattern permitted continuous operation of the one-stage extractor. A separate tank was provided as a surge tank for the aqueous salt solution required for the introduction of the transient concentration signal.

The return lines from the decanter to the aqueous- and organic-phase surge tanks were provided with divert lines to separate tanks so that once the input signal of aqueous salt concentration was started, the discharge streams could be diverted from the surge tanks.

To determine the effect of tank geometry two different size tanks were used for the extraction stage. The first tank had an inside diameter of 11⅜ in. and was equipped with four stainless steel vertical baffles spaced 90 deg. apart. The baffle width was 1/10th of the inside diameter of the agitated contractor. The agitator was a flat bladed turbine type containing six blades. An 8-in. diameter turbine was used for some experimental runs and a 4-in. diameter turbine for others in conjunction with the 11⅜-in. diameter tank. The relative dimensions of all the turbine impellers used in the study followed the suggestion of Rushton et al. (*17*). In all the experimental runs the impeller was positioned at the elevation of the liquid-liquid interface in the extractor when agitation was discontinued and the phases permitted to separate.

A second smaller diameter agitated tank having the same basic construction as the first was used for some experimental runs. The inside diameter of this tank was 5-9/16-in.

The agitator shaft was driven by a 1/3 hp. variable speed motor. The impeller speed could be varied over a continuous range of 0 to 500 rev./min.

The temperature in the agitated contactors was controlled by varying the current in a set of nichrome wire heaters on the aqueous- and organic-phase feed pipes. The equipment was heavily insulated to keep heat losses to a minimum.

The interfacial area of the agitated phases in the contactor was determined from light transmission measurements by the

method of Rodger (*15*), based on the fact that the light transmitted through a poly-dispersed system of transparent isotropic particles is a function of the total projected area. Therefore this transmitted light can be correlated to the interfacial area. The light transmission measurement apparatus and techniques are described in detail by Trice and Rodger (*20*).

EXPERIMENTAL PROCEDURE

The experimental extractor was first operated continuously on the two-phase system at constant flow rates until saturation of the respecive phases was achieved and steady state conditions were attained. The temperature in the contactor was carefully controlled at 25.0 ± 0.2°C., and feed flow rates of the phases were controlled at the required values for a particular experimental run.

The feed of aqueous phase was then suddenly replaced by an equal flow of aqueous phase of a higher solute concentration which was saturated with the organic solvent. This was accomplished by the proper valve manipulations to connect the tank containing the aqueous solute solution to the aqueous-phase feed pump in place of the saturated aqueous-phase feed tank (see Figure 4). The time of aqueous feed tank change was defined as $t = 0$ for the transient response analysis. The aqueous- and organic-phase discharges were immediately diverted from the feed tanks to the respective discard tanks. This prevented the return of solute to the feed tanks which would cause a variation in feed concentration to the contactor.

Simultaneously samples were taken to the feed streams to the contactor, the two phases in the contactor, and the aqueous phase in the contactor. These samples were taken at periodic time intervals during the experimental run. For most of the runs the duration of the transient period was about 30 min.

The two-phase system in the contactor was sampled with a 100 cc. hypodermic needle, the sample being withdrawn in about 2 to 3 sec. The phases immediately started separating in the hypodermic cylinder into an aqueous phase, a separating middle section, and an organic phase. The aqueous and organic phases were discharged into two separate sample bottles, while the separating middle phase was discarded.

As the two-phase sample was being taken with the hypodermic needle, a simultaneous aqueous phase was withdrawn from the continuous contactor. This was accomplished by use of a vacuum manifold and porous filter stones. The porous filter stone was preferentially wetted by aqueous phase. At low flow rates through the stone it would pass aqueous phase and stop organic phase.

It was found that the 2 to 3 sec. required to sample the two-phase system with the hypodermic needle permitted withdrawal of about 2 cc. of aqueous phase without pulling through organic phase. The manifold valve was then closed and the sampling tube withdrawn from the contactor. This sampling device served as a check on the hypodermic sample, determining whether appreciable interphase mass transfer occurred in the hypodermic tube. It was found that the time constant associated with the time of sampling was sufficiently short with

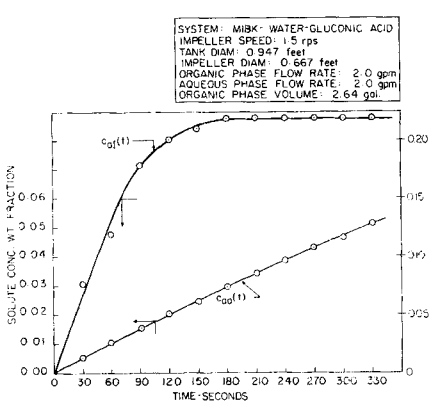

Fig. 5. Example experimental run, aqueous phase.

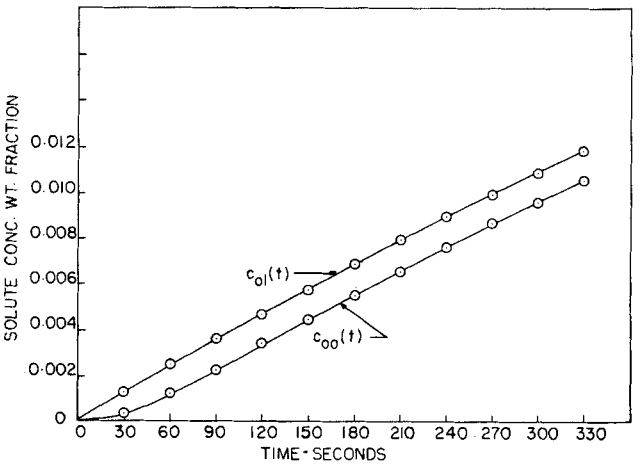

Fig. 6. Example experimental run, organic phase.

respect to the time constant of the diffusion process so that the diffusion occurring in the sample tube could be neglected.

The runs were concluded when the feed tanks were emptied. Interfacial area determinations were made at frequent intervals during the run.

Three solvent systems and three solutes were studied. The solvent systems were chosen on the basis of covering a relatively large range of physical properties belived to be important to this investigation. The solvent systems chosen were methyl isobutyl ketone-water, isoamyl alcohol-water, and cyclohexane-water.

The choice of the solutes was limited by the need for sufficient solubility in both the organic and the aqueous phases of the solvent systems. It was also important that the solutes did not cause a stable emulsion formation between the aqueous and the organic phases of the solvent system. The three solutes chosen were citric acid, maleic acid, and gluconic acid.

ANALYSIS OF RESPONSE FUNCTIONS

The experimental runs involved first running under continuous steady state operation of the two-phase system and permitting the phases to equilibrate. In some runs this equilibration period involved mutually saturating the organic solvent and the water, with each phase having zero solute concentration. In other runs there was an equilibrium established between the phases at a known solute concentration. The solute concentration in the organic phase at equilibrium before the transient period is designated C_b. The solute concentration in the aqueous phase in equilibrium with C_b is designated C_f.

The concentration of solute in the aqueous feed stream was suddenly changed to a higher level. The time of the change was the start of the transient run and defined $t = 0$. Figures 5 and 6 show a typical set of experimental results from a single run with C_b and C_f equal to zero.

The concentration responses of the system for $t > 0$ were designated as follows:

$C_{aI}(t)$ = the concentration of solute in the aqueous feed to the agitated contactor as a function of time.

$C_{ao}(t)$ = the concentration of solute in the aqueous phase in the contactor as a function of time.

$C_{oI}(t)$ = the organic phase solute concentration in equilibrium with $C_{ao}(t)$; from equilibrium data, $C_{oI}(t) \rightleftarrows C_{ao}(t)$.

$C_{oo}(t)$ = the concentration of solute in the organic phase in the contactor as a function of time.

The organic phase in the contactor was considered the system; $[C_{oI}(t) - C_b]$ was regarded as the system input signal. The response of the organic phase to this input signal was $[C_{oo}(t) - C_b]$. This concept in-

volves considering the concentration driving force $[C_{oI}(t) - C_b]$ for diffusion as the input signal imposed on the system by the presence of the aqueous phase concentration $C_{ao}(t)$. The time axis was then divided into equal intervals Δt and the value of $[C_{oI}(t) - C_b]$ and $[C_{oo}(t) - C_b]$ listed for each value of Δt. Equation (20) was then used to calculate the approximation of the system unit impulse response function $\bar{g}_{oo}^*(n\Delta t)$.

A smooth curve was drawn through the approximation values of $\bar{g}_{oo}^*(n\Delta t)$ giving the unit impulse response function $\bar{g}_{oo}(t)$. The bar is written over $g_{oo}(t)$ to indicate that this function describes the average response of the entire organic phase to the input function and therefore does not consider the residence time distribution function of the system. The result of this computation for the example experimental run illustrated in Figure 5 is shown in Figure 7.

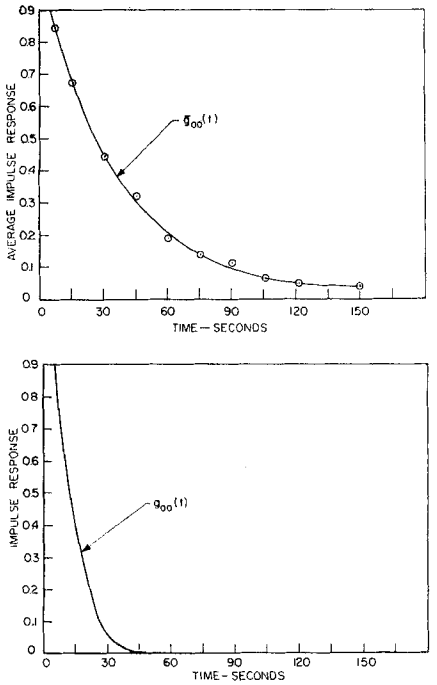

(Top) Fig. 7a. Average organic phase impulse response. (Bottom) Fig. 7b. Organic phase impulse response.

$\bar{g}_{oo}(t)$, the average response of the organic phase to a unit impulse change in the equilibrium value in the agitated contactor, is composed of the total of the responses of the individual differential volumes making up the organic phase. In the case of an agitated tank under continuous flow conditions the residence time of the material in the tank is not uniform. Each differential volume of organic phase is responding to the step change in equilibrium value which produces $\bar{g}_{oo}(t)$. At the start of the transient period $t = 0$ each differential volume starts responding according to the system impulse response function designated $g_{oo}(t)$. Some of the organic and aqueous phases are in the contactor a relatively short time, reaching a residence time of t_1' and a concentration of $g_{oo}(t_1')$, while some are in longer achieving a residence time of t_2' and reaching the concentration $g_{oo}(t_2')$.

In the case of an agitated tank where conditions of perfect mixing can be assumed the residence time distribution function of the organic phase is given by

$$I(t') = (v_o/V_o)\, e^{-v_o t'/V_o} \tag{22}$$

Since the residence time distribution function is a probability distribution, it is independent of the time axis. The residence time distribution does not contribute to the response of the organic phase for $t < t'$. Therefore t' and t represent corresponding time on the time axis, and Equation (22) can be written as

$$I(t) = (v_o/V_o)\, e^{-v_o t/V_o} \tag{23}$$

The function $\bar{g}_{oo}(t)$ represents a summation of the individual differential element impulse responses according to the function $g_{oo}(t)$ weighted by the residence distribution function as follows:

$$\bar{g}_{oo}(t) = \frac{\int_o^t g_{oo}(t) e^{-[(v_o/V_o)t]} dt}{\int_o^t e^{-[(v_o/V_o)t]} dt} \tag{24}$$

Solving for $g_{oo}(t)$ one obtains

$$g_{oo}(t) = \bar{g}_{oo}(t) + (V_o/v_o)\,(e^{(v_o/V_o)t} - 1)\bar{g}'_{oo}(t) \tag{25}$$

Equation (25) was used to determine the system impulse response function $g_{oo}(t)$ for each experimental run. This function was used in Equation (13) to determine the frequency response function $\bar{H}(jw)$, the computation being performed on the special purpose analogue computer. The frequency response function data were then converted to the system transfer function with the properties of the Bode diagram. The results of these computations for the example experimental run of Figures 5 and 6 are shown in Figure 7 and Table 1.

Table 1

t	$\bar{g}_{oo}(t)$	$g_{oo}(t)$
5	0.90	0.89
7.5	0.85	0.80
10	0.75	0.68
15	0.68	0.40
22	0.54	0.04
30	0.44	—
45	0.33	—
60	0.20	—
75	0.14	—
90	0.12	—
105	0.07	—
120	0.05	—
150	0.04	—

Effort was then directed toward correlation of the experimental results. The objective of a correlation was to relate the poles of the organic-phase transfer function for liquid-liquid mass transfer in an agitated contactor to the physical properties of the system components and the mechanical configuration. The correlation would necessarily be limited to agitated vessels with the general shape, baffling, and agitator characteristics of the type used in this investigation.

It is emphasized that this basic approach assumed that the mass transport process would be described by a linear differential equation with constant coefficients over the range of concentration variation employed in this study.

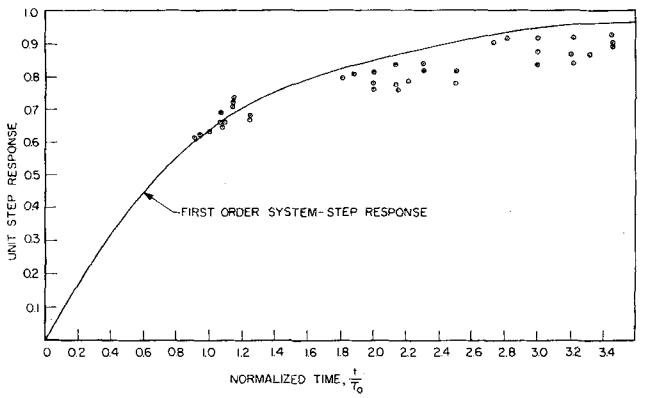

Fig. 8. Normalized step response.

It should be noted that for a contactor under steady flow conditions, $g_{oo}(t)$ is independent of the flow rates when the kinetic energy of the feed streams to the contactor is negligible when compared with the kinetic energy input of the agitator. This is the usual condition for the type of contactor employed in this investigation.

$g_{oo}(t)$ is a function of the physical properties of the system and the factors affecting the agitation characteristics. It should be noted that the volume fraction of organic phase x does not appear in Equation (25). This factor affects $g_{oo}(t)$ only to the extent that it affects the agitation characteristics.

EXPERIMENTAL RESULTS

The frequency response function $\overline{H}(jw)$ was first determined for the systems methyl isobutyl ketone-water-citric acid, methyl isobutyl ketone-water-gluconic acid, and cyclohexane-water-citric acid. All of these systems are characterized by the fact that the solute solubility is extremely high in the aqueous phase and extremely low in the organic phase, the slope of the equilibrium curves being in the range 0.0003 to 0.03. Therefore the resistance to interphase mass transfer is essentially confined to the organic phase. The Bode diagrams for these systems were all approximated by a first-order linear differential equation of the form

$$\frac{dC_{oo}(t)}{dt} + \frac{C_{oo}(t)}{T_o} = \frac{C_{oI}(t)}{T_o} \qquad (26)$$

TABLE 2

System*	T_o, (63.2%)	$(N_{Sc})^{1/2}$	$(N_{Re} \times 10^{-3})$	$\left(\frac{D}{T_o D_o x a}\right)$
c	33	22.2	86.8	2,280
a	32	21.1	82.5	2,180
c	24	22.2	62.4	3,800
g	24	29.4	43.3	2,280
h	6.8	24.4	65.9	3,660
a	28	21.1	24.5	1,340
a	7.5	21.1	51.7	2,390
c	30	22.2	78.0	2,520
g	14	29.2	50.3	3,350
g	13	29.4	55.6	3,220
g	13	29.2	62.9	2,930
h	13	25.2	55.9	2,210
h	14	24.4	54.0	2,400
h	30	25.2	43.5	1,250

* System key: a = MIBK-water-citric acid, c = MIBK-water-gluconic acid, g = cyclohexane-water-citric acid, h = cyclohexane-water-maleic acid.

where T_o represents the time constant, or 63.2% step response time, of the system. The computed normalized step response functions for the four systems are shown in Figure 8 compared with the normalized first-order step response curve for Equation (26). The maximum deviation from the normalized first-order step response is 12%. The values of time constant for the various experimental conditions imposed on the system are shown in Table 2.

Since the reciprocal of the time constant is related to the overall mass transfer coefficient of the system, it was anticipated that a correlation of liquid-liquid overall mass transfer coefficients might be employed to correlate the data.

When the aqueous-phase film resistance is negligible, the diffusion of solute A across the organic-phase stagnant film adjacent to the interface is given by

$$N_{Ao} = ak_{Ao}\,(C_{oI}(t) - C_{oo}(t)) \qquad (27)$$

Comparison of Equation (27) with Equation (20) gives the relationship between the first-order system time constant T_o and the mass transfer coefficient as

$$k_{Ao} = \frac{1}{T_o x a} \qquad (28)$$

In a study of mass transfer including transfer between two immiscible liquids Rushton (17) suggested a correlation of the form

$$(N_{Sh})\,(N_{Sc})^{-s} = f(N_{Re}) \qquad (29)$$

The Higbie-Danckwerts (6) penetration theory postulates that the mass transfer coefficient should be proportional to the square root of the molecular diffusivity suggesting a value of ½ for s in Equation (29).

Equation (28) was substituted for the mass transfer coefficient in the Sherwood number in Equation (29), and the experimental results were correlated by the following equation:

$$\left(\frac{D}{D_o T_o x a}\right)\left(\frac{\mu_o}{\rho_o D_o}\right)^{-1/2} = K_o\left(\frac{D^2 N_{po}}{\mu_o}\right)^{b_o} \qquad (30)$$

The results of this correlation attempt are shown in Figure 9. The best line through the correlation gave the following results:

$$K_o = 10$$

$$b_o = 0.6$$

The maximum deviation from the correlation curve is approximately 40%.

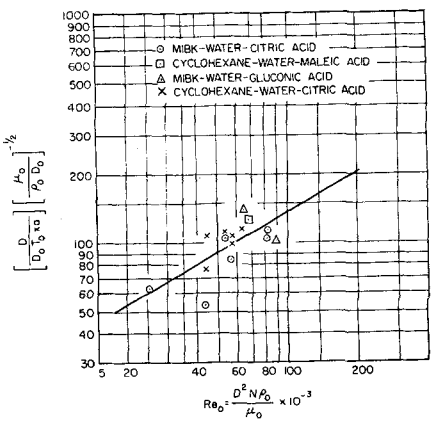

Fig. 9. Time constant correlation for organic phase.

The frequency response function $\overline{H}(j\omega)$ was then determined for the systems methyl isobutyl ketone-water-maleic acid, isoamyl alcohol-water-maleic acid, and isoamyl alcohol-water-citric acid for the various experimental conditions employed in this study. In these systems the resistance to solute diffusion involved a series system with some resistance on each side of the interface. When the frequency response function was determined by Equation (13), the result indicated a system of order greater than 1 in the majority of cases.

The usually accepted model of interphase mass transfer involving two film resistances on each side of the interface and no resistance of the actual interface is summarized by the block diagram of Figure 10, where $C_{ai}(t)$ and $C_{oi}(t)$ are the interface compositions of the aqueous and organic phases respectively.

With the assumption of constant mass transfer coefficients over the concentration ranges employed in the transient runs, the film resistance blocks are linearized elements and can be characterized by transfer functions. For the systems employed in this study the equilibrium curve could be approximated by a straight line through the origin, resulting in a linearization of the equilibrium block. Since the order of the blocks is of no consequence in a linear series system, the block diagram of Figure 10 can be represented for this case as the block diagram of Figure 11.

The phase compositions at the interface have been eliminated by considering the two film resistances as a second-order cascade. This approach suggests that the process would be a second-order system containing two real roots. The linear differential equation describing this system is of the form

$$\frac{d^2C_{oo}(t)}{dt^2} + \left(\frac{1}{T_o} + \frac{1}{T_a}\right)\frac{dC_{oo}(t)}{dt} + \frac{C_{oo}(t)}{T_oT_a} = \frac{C_{oI}(t)}{T_oT_a} \tag{31}$$

where T_o and T_a represent the time constants or 63.2% step response times of the respective organic- or aqueous-phase systems. It was assumed that departures from a second-order system were the result of errors, and the two dominant roots were used to characterize the system.

Since the dynamic analysis of a series linear system does not distinguish between the order of resistances, it was necessary to consider additional information to make the decision on which root was attributable to each of the two phase resistances on the basis of their respective magnitudes. This information was provided by considering the slope of the solute solubility equilibrium curve which suggested which of the film resistances was the larger. This decision was checked by testing the time constant ascribed to the organic phase against the correlation Equation (30).

The results of these computations are summarized in

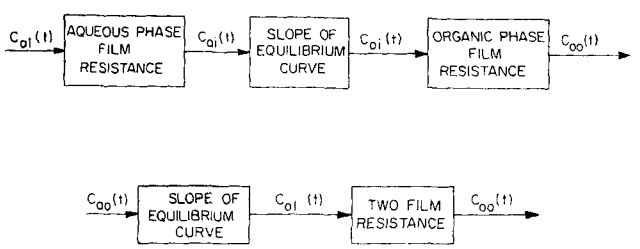

(Top) Fig. 10. Block diagram of interphase mass transfer. (Bottom) Fig. 11. Block diagram, linear interphase mass transfer.

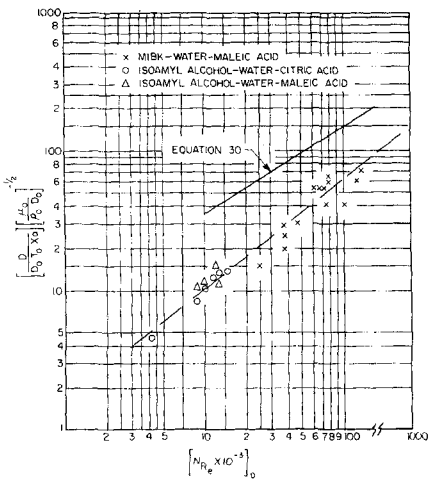

Fig. 12. Time constant correlation, organic phase.

Table 3.* The organic-phase time constants for these systems were then plotted and compared with correlation Equation (30) in Figure 12. The values of K_o and b_o for the best correlation curve for the second-order systems organic-phase time constant data are

$$K_o = 1.8$$

$$b_o = 0.8$$

The value of b_o compares favorably with the value obtained from the first-order systems; however the value of K_o exhibited a shift from the previous value of 10. The significance of this shift is not apparent, emphasizing the need for additional experimentation. The maximum deviation from the best correlation curve for the second-order system is approximately 30%.

A similar correlation was attempted with the time constants attributed to the aqueous-phase film resistances. The correlation equation for the aqueous phase is given by

$$\left(\frac{D}{D_aT_axa}\right)\left(\frac{\mu_a}{\rho_aD_a}\right)^{-1/2} = K_a\left(\frac{D^2N\rho_a}{\mu_a}\right)^{t} \tag{32}$$

The results of this correlation effort are shown in Figure 13. The best line through the correlation curve gave the following results:

* Tabular material has been deposited as document 7762 with the American Documentation Institute, Photoduplication Service, Library of Congress, Washington 25, D. C., and may be obtained for $1.25 for photoprints or for 35-mm. microfilm.

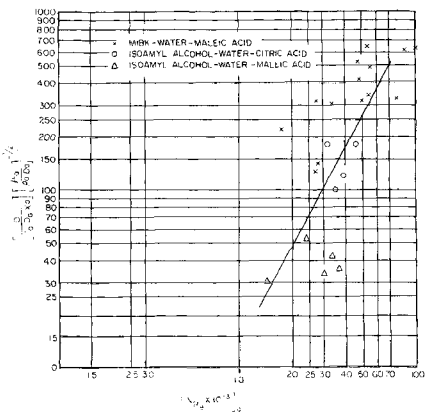

Fig. 13. Time constant correlation, aqueous phase.

$$K_a = 0.03$$

$$f = 1.8$$

The scatter about the correlation curve is considerable; however the correlation is statistically significant. The maximum deviation from the correlation is approximately 90%. The major factor causing errors in the determination of the aqueous-phase time constants is associated with the problem of determining the second, and considerably smaller, root of the second-order system from the experimental data.

Duplicate runs showed a reproducibility of T_o for the first-order systems of 8%, T_o for the second-order systems of 9%, and T_a for the second-order systems of 12%.

SUMMARY AND CONCLUSIONS

Interphase mass transport has been studied with a systems approach to the problem of characterization of the process. The systems and concentrations employed in this investigation permitted use of a linearized model. The time constants of the system were determined and related to the mass transfer coefficients.

An attempt was made to correlate the results by techniques which have enjoyed some success in correlating mass transfer coefficients. The results were not successfully correlated by this approach.

The results of transient tests are strongly influenced by the behavior of the system in the neighborhood of the starting time $t = 0$. It is suggested that continuous analysis techniques be employed in future investigations of this type rather than the discrete sampling approach used in this investigation to reduce errors in the vicinity of the origin.

ACKNOWLEDGMENT

The major part of the equipment and instruments were provided by the Argonne National Laboratory. Dr. Walter Rodger, Associate Director of *Chemical Engineering*, has given valuable advice and encouragement. Grateful acknowledgment is made to Dr. Rodger and Argonne National Laboratory.

NOTATION

a = interfacial area per unit volume of total mixed phase, sq.ft./cu.ft.
C = concentration of solute in a phase, lb./lb. of phase
C_b = steady state concentration of solute in organic phase, lb./lb. of phase
C_f = steady state concentration of solute in aqueous phase, lb./lb. of phase
D = impeller diameter, ft.
D_v = molecular diffusivity, sq.ft./sec.
D_a = molecular diffusivity of solute in aqueous phase sq.ft./sec.
D_o = molecular diffusivity of solute in organic phase sq.ft./sec.
$g(t)$ = unit impulse response of system
k_A = individual mass transfer coefficient in the aqueous phase, ft./sec.
k_O = individual mass transfer coefficient in the organic phase, ft./sec.
N = impeller speed, rev./sec.
N_A = rate of mass transfer, lb./sec.
N_{Sh} = Sherwood number
N_{Sc} = Schmidt number
N_{Re} = Reynolds number
s = Laplace operator
t = time, sec.
t' = time in contactor (residence time), sec.
T = system time constant, sec.
$u(t)$ = unit step function
$u_\epsilon(t)$ = approximate unit step function
$w(t)$ = unit step response of system
x = volume fraction of organic phase
z = polynomial operator

Greek Letters

ρ = density, pounds/cu.ft.
μ = viscosity, pounds/ft.sec.
$\delta(t)$ = unit impulse function
$\delta_\epsilon(t)$ = approximate unit impulse function
$\theta_i(s)$ = Laplace transform of $\theta_i(t)$
$\theta_0(s)$ = Laplace transform of $\theta_0(t)$
$\theta_i(t)$ = input signal to system
$\theta_0(t)$ = corresponding output signal to input $\theta_i(t)$
$\Phi(D)$, $\xi(D)$ = polynomials in D operator, characteristic of system

Subscripts

a = aqueous phase
o = organic phase
I = input
o = output (when used as a second subscript)
aI = aqueous phase input
ao = aqueous phase output
oI = organic phase input
oo = organic phase output
i = interface condition

Superscripts

$*$ = approximation of function

LITERATURE CITED

1. Acton, F. S., and Leon Lapidus, *Ind. Eng. Chem.*, **47**, 706 (1955).
2. Bode, H. W., "Network Analysis and Feedback Amplifier Design," D. Van Nostrand, New York (1945).
3. Baber, M. F., L. L. Edwards, Jr., W. T. Harper, Jr., M. D. Witte, and J. A. Gerster, *Chem. Eng. Progr. Symposium Ser. No. 36*, **57**, p. 148 (1961).
4. Boothroyd, A. R., E. C. Cherry, and R. Makar, *Proc. Inst. Elec. Engrs.* Part I, **96**, pp. 163-177 (May, 1949).
5. Danckwerts, P. V., *Chem. Eng. Sci.*, **2**, 1 (1953).
6. ———, J. W. Jenkins, and G. Place, *Chem. Eng. Sci.*, **3**, 26 (1954).
7. Deisler, P. F., and R. H. Wilhelm, *Chem. Eng. Progr.*, **49**, 150, (1953).
8. Ebach, E. A., and R. R. White, *A.I.Ch.E. Journal*, **4**, 161 (1958).
9. Evans, W. R., *Trans. Am. Inst. Elec. Engrs.*, **67**, pp. 547-551 (1948).
10. Fowler, F. C., and G. G. Grown, *Trans Am. Inst. Chem. Engrs.*, **39**, 491 (1943).
11. Gilliland, E. R., and E. A. Mason, *Ind. Eng. Chem.*, **41**, 1191 (1949).
12. *Ibid.*, **44**, 218 (1952).
13. McKnight, G. W., and C. W. Worley, *Paper No. 56-6-1*, presented at Eighth National Conference of ISA (Sept., 1953.)
14. McHenry, K. W., Jr., and R. H. Wilhelm, *A.I.Ch.E. Journal*, **3**, 83 (1957).
15. Rodger, W. A., V. G. Trice, Jr., and J. H. Rushton, *Chem. Eng. Progr.*, **52**, 515 (1956).
16. Rosen, J. B., and R. Winsche, *Chem. Phys.*, **18**, 1587 (1950).
17. Rushton, J. H., *Chem. Eng. Progr.*, **47**, 485 (1951).
18. Rosenbrock, H. H., *Trans. Inst. Chem. Engrs. (London)*, **35**, 347-51 (1957).
19. Solodovnikov, V. V., "Introduction to the Statistical Dynamics of Automatic Control Systems," Dover Publications (1960).
20. Trice, V. J., Jr., and W. A. Rodger, *Argonne Natl. Lab. Rept. ANL-5512* (1956).

Manuscript received December 21, 1962; revision received July 18, 1963; paper accepted July 23, 1963.